Nanoparticles magnetization switching by Surface Acoustic Waves

Author: Júlia Tena Vidal
Facultat de Física, Universitat de Barcelona, Diagonal 645, 08028 Barcelona, Spain.

Advisor: Javier Tejada Palacios

Abstract: In this project we present a simulation which allows the prediction of the spin-phonon interaction in magnetic nanoparticle samples. The study of new techniques to manipulate the magnetic moment of nanostructures are being increasingly demanded [1–5]. For this purpose, surface acoustic waves (SAWs) are excellent candidates since they offer a dynamic and tuneable mechanism for the control of low energy excitations. The goal of the project is to better understand the mechanism of magnetization switching produced by SAWs, developing a numerical solution of the theoretical model previously proposed by Professor Eugene M. Chudnovsky [6]. We have developed our theoretical calculations used to predict the magnetization jump dependency on different parameters such as system temperature, SAWs power and frequency and sample magnetic properties. Some of these dependencies have been experimentally verified using a Superconducting Quantum Interference Device magnetometer (SQUID) at the Laboratory of Magnetism and Superconductivity of the University of Barcelona.

I. INTRODUCTION

Magnetic single domain nanoparticles (NPs) are a hot topic due to the wide range of applications (medical applications, sensors, electronic devices...) and the interest in low dimensional systems from a fundamental point of view. There is an increasing interest in modifying the magnetic moment of NPs and SAWs are an excellent mechanism to do it since they are easy to use and offer a dynamic and tuneable mechanism for the control of low energy excitations.

Surface acoustic waves (SAWs) [3, 4] are elastic deformations propagating along the surface of an elastic body, in our case a piezoelectric material $LiNbO_3$. Thus, they carry both an elastic wave and a voltage wave in the material. Since their amplitude decays rapidly into the bulk, the acoustic energy which is carried by the SAW is highly confined in a depth of around one wavelength below the surface.

The interaction of SAWs with magnetic materials like ferromagnetic layers has been studied in recent years [2, 4, 6]. However, previous studies does not provide accurate explanation of the magnetization jump when applying SAWs at certain conditions. In our case, and according to theoretical model of Professor Eugene M. Chudnovsky [6], we will provide deeper understanding of this phenomenon by means of developing a numerical solution of his model. We have demonstrated that the theoretical solution of our numerical solution explains preliminary experimental results properly. We propose new ways to optimize the magnetization jump which could be used in future applications.

II. SAMPLE CHARACTERIZATION

Ferromagnetic bulk contains different regions called *magnetic domains* in which the angular momentum, spin direction of the atoms have the same orientation. In a bulk ferromagnet, domains have different orientations of the total magnetic moment in order to minimize the energy of the system, resulting therefore, in a null net moment.

Magnetic domains have a sizes depending on the used material because it depends on the domain wall. A*single domain nanoparticle (NPs)* is a nanometrical part of the material having a net magnetic moment different to zero.

The samples used in experiments are formed by spherical NPs, also called particles in this report. An ideal sample would only contain single-size nanoparticles, but this has not already been achieved, and a particle size distribution with a diameter variation around 10 nm can be found in the sample.

In order to characterize the NPs, it is important to carry out measurements like ZFC-FC, AC susceptibility and isothermal magnetization curves.

A. Magnetic susceptibility

The sample is formed by a set of particles with the same volume (V) at a temperature (T). An alternating (AC) magnetic field with angular frequency (ω) is applied to the sample. The real $\chi^{'}$ and imaginary part $\chi^{''}$ of the AC susceptibility are defined as [7]:

$$\chi^{'}(V,\,T,\,f) = \chi_0 \frac{1}{1+(\omega\tau)^2} \tag{1}$$

$$\chi^{''}(V,\,T,\,f) = \chi_0 \frac{\omega\tau}{1+(\omega\tau)^2} \tag{2}$$

where χ_0 is the equilibrium magnetic susceptibility and can be calculated as follows:

$$\chi_0 = \frac{M_S^2 V}{3\kappa_B T} \tag{3}$$

Being M_S the sample's magnetization, κ_B the Boltzmann constant and K the sample anisotropy constant.

χ'' peaks at $\omega = 2\pi f = 1/\tau$, angular frequency in which the particles absorb the maximum (magnetic field) energy. τ is the spin-switching time ($|\uparrow\rangle \longleftrightarrow |\downarrow\rangle$) of the particle which is given by:

$$\tau = \tau_0 \exp\left\{\frac{KV}{\kappa_B T}\right\} \tag{4}$$

τ_0 is the attempt time to cross the energy barrier, which is usually of the order of nanoseconds. In the case we have a volume distribution $f(V)$ instead of single size particles, equations (1) and (2) can be stated as:

$$\chi' = \frac{\chi_0}{V_{Tot}} \int_0^\infty dV\, f(V)\, V \frac{1}{1+(\omega\tau)^2} \tag{5}$$

$$\chi'' = \frac{\chi_0}{V_{Tot}} \int_0^\infty dV\, f(V)\, V \frac{\omega\tau}{1+(\omega\tau)^2} \tag{6}$$

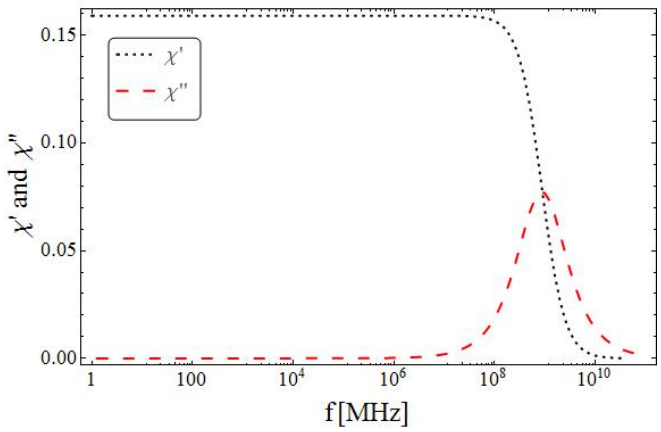

FIG. 1: Magnetic susceptibility for a Gaussian distribution function with mean value of 5nm 15%.

According to experimental measurements, and as a first approach, the diameter distribution of the sample $g(\phi)$ for our calculation is considered Gaussian, see Fig. 2. $f(V)$ can be easily calculated from (ϕ) considering spherical particles [7].

B. Zero Field Cooled and Field Cooled curves

The *Zero Field Cooled (ZFC)* and *Field Cooled (FC) curves* correspond to the metastable and stable states of the system under an applied magnetic field at different temperatures. In order to characterize a magnetic sample these curves have to be obtained.

The experimental protocol to measure the ZFC curve is [4, 7, 8]:

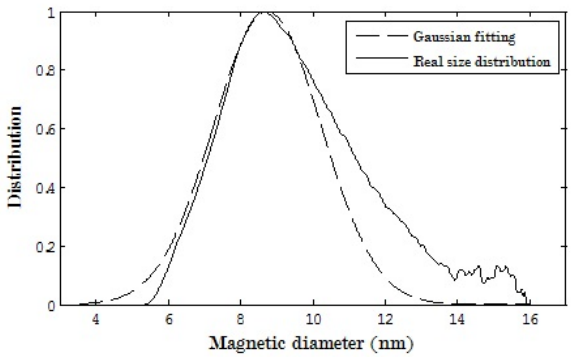

FIG. 2: Size distribution of the sample calculated from the ZFC and FC curves using Eq. (11). @ Gaussian function parameters: $\mu = 8.74\,\text{nm}$ and $\sigma = 1.5\,\text{nm}$

1. The system is cooled from room temperature to 5K without a magnetic field applied.
2. A magnetic field H much more smaller than the anisotropy field $H_A = \frac{2K}{M_S}$ is applied.
3. The sample is warmed up under the presence of a magnetic field in order to measure the magnetization dependence on temperature.

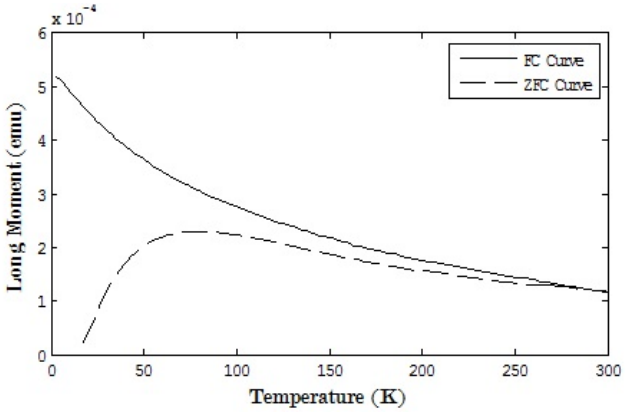

FIG. 3: ZFC and FC curves experimentally calculated for the sample considered in Fig.1. ZFC and FC should coincide in the case the sample's temperature is above the blocking temperature because the system is in equilibrium. However, in real systems this is not true due to the dipolar interactions between particles. @ $T_B \approx 60K$.

(Step 1) At room temperature and without influence of magnetic fields, the easy axes of the particles are randomly oriented. Hence, the total magnetization of the sample $\mathcal{M}$ becomes null. The consequence of cooling down the sample is that the spin of the particles is blocked in its previous state randomly. Consequently, the total magnetic moment remains zero at zero field.

(Step 2) Due to the applied magnetic field, the energy barrier U between up and down states is modified. In this

situation one of the two states is more stable and spin of particles can easily jump the energy barrier when *(Step 3)* the temperature is sufficiently increased. The probability of jumping the energy barrier is directly correlated with the particle's volume and is given by the Arrehnius law [7, 9]:

$$\Gamma = \nu_0 \exp\left\{-\frac{U}{\kappa_B T}\right\} \tag{7}$$

with U being the anisotropy barrier, $U = KV$, and ν_0 the attempt frequency, $\nu_0 = 1/\tau_0$. The smaller the particles, the lower the energy needed to jump the barrier. Particles behave superparamagnetically if the temperature of the sample is higher than the *blocking temperature* (T_B), stated as [7, 9]:

$$T_B = \frac{U}{\kappa_B \ln \nu_0 \tau_m} \tag{8}$$

where $\tau_m = 1/\Gamma$ is the measuring time.

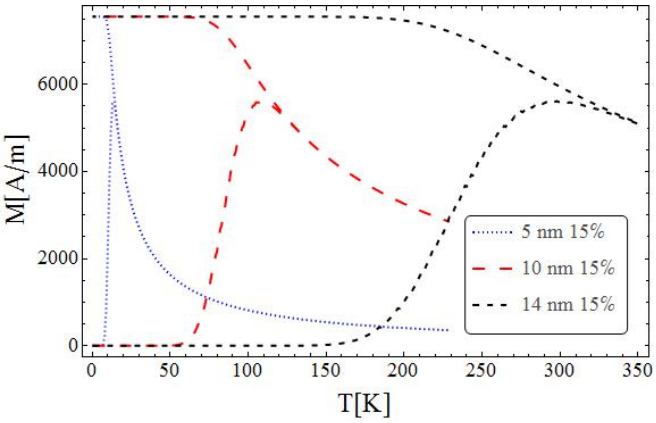

FIG. 4: Numerical ZFC and FC curves for different Gaussian functions with a standard deviation of 15%. The blocking temperature of each sample is the maximum of the ZFC curve.

In a similar way we can define the *blocking volume* [7, 9]:

$$V_B = \frac{\kappa_B T}{K} \ln \nu_0 \tau_m \tag{9}$$

If the volume particle is bigger than the blocking volume, $V > V_B$, the magnetic moment of the particle cannot change its state, i.e. the particles are "frozen". Otherwise, their magnetic moment obeys the Curie-Weiss Law for superparamagnets.

The ZFC curve has a broad maximum corresponding to the broad distribution of sizes. The largest particles determine the blocking temperature of the system because of their dominating contribution to the total magnetization. This case corresponds to the majority of the magnetic moment all particles are oriented along the direction magnetic field. Due to thermal effects, which cause a random shifting of the spin moment, increasing the temperature, the magnetization goes to zero.

For $T > T_B$, the system is in the equilibrium following the FC curve and magnetization of the system behaves as Curie Law predicts.

Experimentally, the FC is obtained by measuring sample's magnetization while cooling the system from room temperature to low temperatures applying a magnetic field H smaller than H_A. In this case, the anisotropy barrier will remain deformed and the particles would be able to change its spin even if $T < T_B$.

In our simulations, we use the mathematical model of ZFC curve [7, 9],

$$m_{ZFC} = \frac{M_S^2 H \mu_0}{2\kappa_B T} \int_0^{V_B(T,t)} dV\, f(V)\, V^2 \tag{10}$$

For the case of the FC curve corresponds to the equilibrium magnetization and, therefore, the magnetization decreases as $1/T$.

With the ZFC and FC curves of a sample, its particle diameter distribution ($g(\phi_B(T))$) can be calculated using:

$$g(\phi_B(T)) = \frac{1}{\alpha} T^{2/3} \frac{d\mathcal{M}_{FC-ZFC}}{dT} \tag{11}$$

and

$$\alpha = -\frac{M_S^2 H \mu_0}{2\kappa_B} \frac{1}{3} \left(\frac{6}{\pi}\right)^{\frac{1}{3}} \left(\frac{\kappa_B \ln \nu_0 \tau_m}{K}\right)^{\frac{4}{3}} \tag{12}$$

As an example, from experimental ZFC and FC curves, see Fig.3, we have obtained $g(\phi)$, see real size distribution in Fig.2.

III. MAGNETIZATION SWITCHING BY SAWS

This section is intended to study the behaviour of a set of nanosize magnetic material under the influence of SAWs [2, 6].

The main consequence of applying SAW to a sample is a perturbation propagating trough the crystal which creates a rotation of the entire matrix. Due to momentum conservation, the particles of the sample must begin rotate, creating a magnetization jump ΔM in the quasi-equilibrium magnetization $M_{eq}(T)$, or in other words, a change in the net magnetic moment, see Fig.5.

The equilibrium magnetization M_{eq} is the Field Cooled curve after the field generated by the SAW is switched off. For the sake of simplicity, in the program the FC curve is approximated to Curie-Weiss Law.

Considering a small change in the magnetization, $\Delta M \ll M_{eq}$, the jump in magnetization due to SAW is [6]:

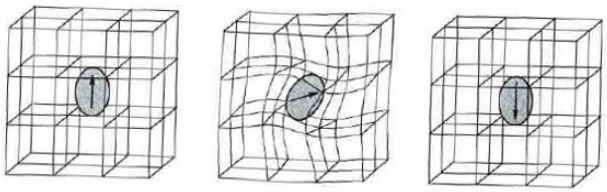

FIG. 5: Magnetization jump of a single-domain particle embedded within an elastic matrix due to the propagation of SAWs through the sample [8]. In real time the particle goes directly from the state (a) to the state (c).

$$\Delta M \propto f^3 P_{SAW} \left(\frac{\partial M_{eq}}{\partial T}\right) \frac{\partial}{\partial T} \int dV\, f(V) \chi''(V,T,f) \tag{13}$$

where P_{SAW} is the wave power in dB.

Thus, ΔM shows the numbers of blocked particles which have been able to cross the barrier with the help of SAWs.

Equation (13) has been solved using numerical simulations (Wolfram Mathematica 9.0).

The numerical solution is obtained for a specific volume distribution function, in our case considered Gaussian, see Fig.2.

Firstly, we have analysed the dependence of SAW's power on magnetization jump for two different frequencies. This experiment is interesting because it could be experimentally measured using a SQUID magnetometer.

In experiments we study the magnetization jump dependence on the SAW power for the different frequencies of the piezoelectric material. The numerical solution for different powers is shown at Fig. 6 and the solution shows that the dependency is lineal, as expected by Eq. (13).

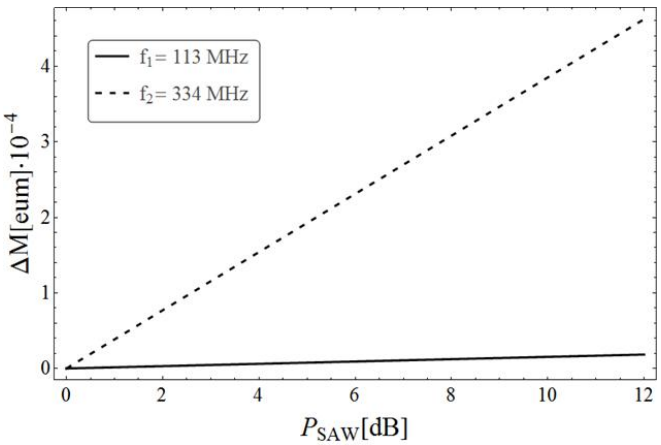

FIG. 6: Magnetization jump dependence on the power of SAW. System temperature T=30K, $P_{SAW} = 6dB$. Size distribution parameters: $\mu = 8.75$nm and $\sigma = 1.5$nm, diameter distribution of Fig. 2.

Fig. 6 depicts that when increasing the SAW's power we increase the magnetization jump but its dependency is amplified for higher frequencies. Since the power SAW dependence present a slight slope and the SAW frequency dependence is close to f^3 (Fig. 7), the magnetization jump is more abrupt for frequency changes rather than for power variations.

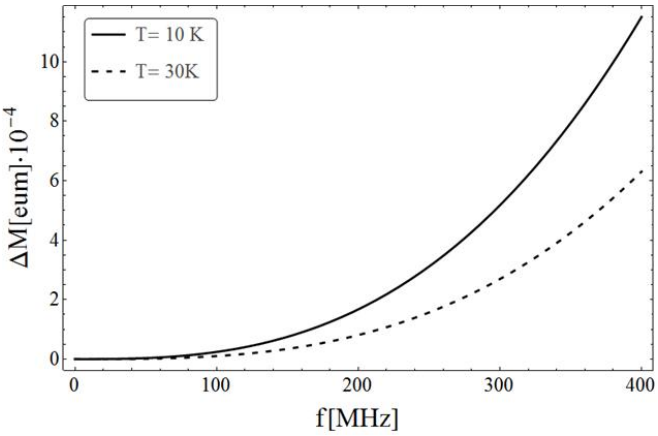

FIG. 7: Magnetization jump dependence on the SAW frequency for two temperatures. Size distribution parameters: $\mu = 8.75$nm and $\sigma = 1.5$nm, $P_{SAW} = 6$ dB.

We can also determine the dependence with temperature, although it is not easy to quantify. A more accurate study is done by using different size distribution samples, see Fig. 8.

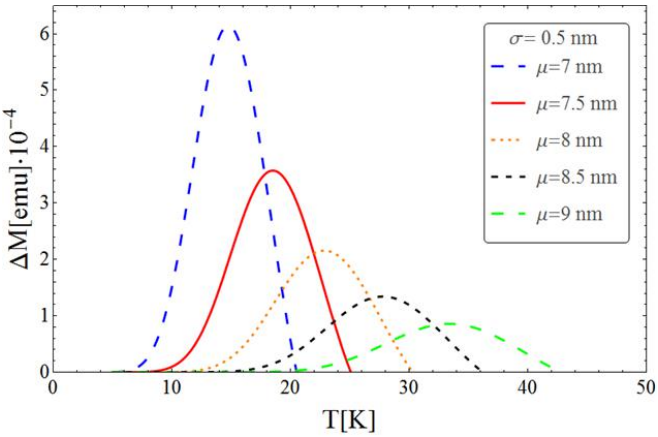

FIG. 8: Magnetization jump dependence on the temperature for different samples. Size distribution with $\sigma = 0.5nm$ when varying the mean value. Sample 1) $T_B \approx 20$K, Sample 2) $T_B \approx 25$K, and Sample 3) $T_B \approx 30$K, Sample 4) $T_B \approx 35$K, Sample 5) $T_B \approx 40$K. $P_{SAW} = 6$dB and $f = 113$MHz.

For a given sample potency and frequency, there is an optimal temperature (T_{opt}) that maximizes the jump. This temperature is always lower than the blocking temperature ($T_{opt} < T_B$). When $T_{opt} = T_B$ the magnetization jump becomes zero. This is because all particles behave as superparamagnets and therefore, SAW can only affect blocked particles.

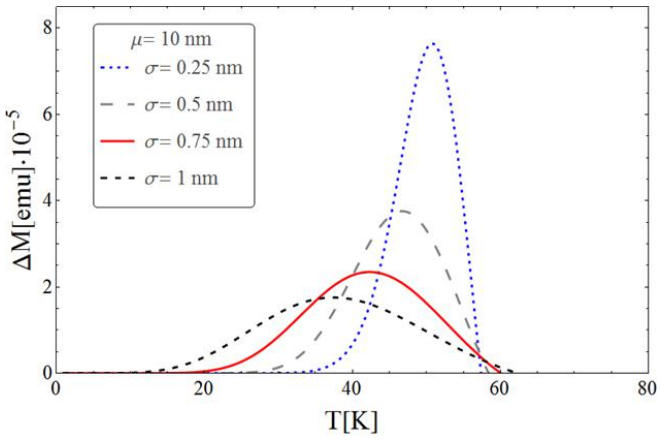

FIG. 9: Magnetization jump dependence on the temperature for different samples. Size distribution with $\mu = 10nm$ when varying σ. Sample 1) $T_B \approx 55$K, Sample 2) $T_B \approx 55$K, and Sample 3) $T_B \approx 60$K, Sample 4) $T_B \approx 60$K. $P_{SAW} = 6$ dB and $f = 113MHz$.

The magnetic jump depends on the number of blocked particles and the anisotropy barrier of each particle (U). For a given temperature, the energy given by SAW goes first to change the magnetic moment of particles with the lower anisotropy barrier, the smallest ones. Bigger particles need more energy to jump and for this reason, less particles would be able to jump the barrier. For higher temperatures (close to T_B) blocked particles are bigger and, for this reason, with the same energy less particles will jump. The optimal temperature is found when we have the maximum number of particles available to maximize the magnetization jump.

In Fig.8 the magnetization jump dependence on temperature is studied for different samples by changing its mean volume. It is observed that by decreasing the mean volume of the sample the magnetization jump increases. Samples with bigger particles need more energy to jump the anisotropy barrier and then, less particles can change their magnetic moment, i.e. the magnetic jump is smaller. Moreover, by decreasing the width of the size distribution the magnetization jump is also increased, see Fig.9.

IV. CONCLUSIONS

In this project a numerical solution for the model [6] is performed to study theoretically the interaction of SAWs with a magnetic sample. We have demonstrated that the magnetization jump increases for higher SAW's frequency and power, and presents a maximum for temperatures below Blocking temperature. The importance of the features of the sample has also been studied, leading to the conclusion that magnetization jump can be maximized for magnetic samples with the smallest mean volume and standard deviation possible. Thus, we present a work which complements Chudvnosky's model and show a way to improve the ability of SAWs to free blocked particles converting them to superparamagnetic particles. This research opens a door towards the tailoring of magnetization jump and gives an insight into the conditions in which SAWs should be used in different applications.

Acknowledgments

I would like to express gratitude to my advisor Dr. Javier Tejada who gave me the opportunity to start working in this promising project, as well as Nahuel Statuto and Jaume Calvo de la Rosa for helping me always I needed. Moreover, thanks Daniel Segura, my family and friends to help me in what they were capable of.

[1] L. Dreher, M. Weiler, M. Pernpeintner, H. Huebl, R. Gross, M. S. Brandt, and S. T. B. Goennenwein. Surface acoustic wave driven ferromagnetic resonance in nickel thin films: Theory and experiment. *Physical Review B*, 86(13):134415, oct 2012.

[2] Eugene M. Chudnovsky and Reem Jaafar. Manipulating the Magnetization of a Nanomagnet with Surface Acoustic Waves: Spin-Rotation Mechanism. *Physical Review Applied*, 5(3):031002, mar 2016.

[3] Martí Checa Nualart. Study of the magnetic properties of nanoparticles interacting with surface acoustic waves. 2015.

[4] Ferran Macià Bros. *Magnetic experiments with surface acustic waves and microwaves*. PhD thesis, Universitat de Barcelona, 2009.

[5] Eugene M. Chudnovsky. Electromechanical magnetitzation switching. *Journal of Applied Physics*, 5(117):103910, mar 2016.

[6] Eugene M. Chudnovsky. *Private Comunication*.

[7] Eugene M Chudnovsky and Javier Tejada. *Lectures on Magnetism*. Rinton Press Paramus, NJ, 2006.

[8] Eugene M. Chudnovsky and Javier Tejada. *Macroscopic Quantum Tunneling of the Magnetic Moment*. 2005.

[9] Jaume Calvo de la Rosa. Measurements of magnetic nanoparticles of molecular magnets. 2014.